

## A Novel Particle Morphological Investigation of Mineral Ore Particles by A Morphologically Directed Raman Spectroscopy

SASAKURA, Daisuke<sup>1\*</sup> ; HAMADA, Hiroyuki<sup>1</sup> ; HAYAUCHI, Aiko<sup>1</sup>

<sup>1</sup>Malvern Instruments, A division of Spectris Co., Ltd.

### [Introduction]

To investigate of the mineral resources as particles such as soil in sea, in ground and in fields is interesting in geochemistry. The existing approach to investigate of mineral resources, the manual microscopic observation method and an elemental analysis technics had been used. The major drawback of a manual microscope approach has been used for few number of particles morphology observation. It is not able to described particle shape as significant number. Furthermore an elemental analysis technique such as X-Ray fluorescence and destructive wet chemical analysis can determine the quantity of mineral species present in the ore, however, these chemical analysis methods do not allow the study of the composition of individual particles of different size and shape. The morphologically directed Raman spectroscopic (MDRS) is a novel approach which can resolve this problem. Using this method the Raman spectra of several hundred particles is determined after size and shape classification of each individual particle by automated particle image analysis. Raman spectroscopy can be used to acquire the spectra of any inorganic compounds such as metal oxides and nitrides which are Raman active. Many mineral resources are mined as inorganic compounds. Therefore, Raman spectroscopy can be used for the identification of the chemical composition of mineral ores. Using the a morphologically directed Raman spectroscopic method described herein, it is possible to calculate the particle size distribution and proportion by mass or volume of each chemical component or mineral species based on Raman spectroscopic information. This study will report and discuss the capability MDRS method using a model material.

### [Material and Method]

These samples had been through the ore dressing process. MDRS measurement was carried out using a Morphologi G3SE-ID instrument (Malvern Instruments, UK) equipped with a dry powder sample dispersion unit (SDU) and Raman module. The laser wavelength of Raman excitation was 785nm the laser power was less than 5mW and the irradiation time was 5 sec. The particle image measurements were made in diascopic mode with a total magnification 250x. Iron ore dry powder samples were dispersed using the SDU using a short duration pulse of compressed air. Measurements were made automatically using Standard Operating Procedures (SOPs) which define the software and hardware settings used. Measurement sample was dispersed on to glass plate as sample carrier which was minimized environmental exposure by the enclosed sample chamber unit. Particle identification by Raman analysis used the spectrum correlation coefficient approach.

Keywords: Particle Size, Particle Shape, Morphology, Raman, Resource analysis

## Raman spectroscopic analysis of carbonaceous material included in oil source rocks

KOUKETSU, Yui<sup>1\*</sup>; OKUMURA, Fumiaki<sup>2</sup>; IWANO, Hirotsugu<sup>2</sup>; WASEDA, Amane<sup>2</sup>; KAGI, Hiroyuki<sup>1</sup>

<sup>1</sup>Geochemical research center, Graduate School of Science, The University of Tokyo, <sup>2</sup>Japan Petroleum Exploration Co.,Ltd. (JAPEX)

Carbonaceous material (CM) included in rocks is important material to produce resources of oil and gas. The quality and storage of these resources are evaluated by analyzing the chemical composition, crystal structure, and reflectance of CM. In the oil exploration, vitrinite reflectance is widely used to evaluate the maturity of CM. However, the spatial resolution of vitrinite reflectance measurement is about 10  $\mu\text{m}$  and more than 100 point measurement is needed for quantitative evaluation. Therefore, the evaluation of maturity of CM is sometimes difficult in low vitrinite content rocks.

In the present study, we examined the maturity of CM using the Raman spectroscopy, whose spatial resolution is about 1  $\mu\text{m}$ . Kouketsu et al. (2014, Island Arc) reported that the values of full width at half maximum (FWHM) of CM Raman spectra correlate with metamorphic temperature and proposed the Raman CM geothermometer. Applicable temperature range is 150 to 400  $^{\circ}\text{C}$  and the reflectance of vitrinite included in the calibrated samples is more than 1 %. We focused on the reflectance less than 1 % where the crude oil is started to produce and carried out the measurement of Raman spectroscopic analysis and reflectance for the samples containing vitrinite grains whose reflectance between 0.25 to 2.44 %.

In the Raman spectroscopic analysis, we used 514.5 nm  $\text{Ar}^+$  laser and set the laser power around 0.2 mW at sample surface to avoid the damage to CM. Measured spectra were divided into four peaks of D1-, D2-, D3-, and D4-bands within the 1000 to 2000  $\text{cm}^{-1}$  range. Raman spectra of CM less than 1 % of reflectance show strong fluorescence background. Raman peaks of CM less than 0.4 % of reflectance cannot be detected. The values of FWHM of D1- and D2-bands vary less than 1 % of reflectance range and the correlation becomes unclear. The CM Raman spectra seem to be affected by the background and peaks are not separated properly. This result indicates that the conventional Raman CM geothermometer is difficult to apply to oil source rocks. On the other hand, the slope of Raman baseline becomes smaller with increasing reflectance, and the correlation is approximated by exponential function. The fluorescence related to the baseline of Raman spectra is considered to be caused by the polycyclic aromatic hydrocarbon that is the main component of oil and gas. Therefore, the baseline slope of CM Raman spectra will be a useful index to evaluate the maturity of oil source rocks.

Keywords: oil source rock, carbonaceous material, Raman spectroscopy, vitrinite reflectance

## Petrological and spacial variations of the near off-axis magmatism controlled by a ridge segment structure

KANEKO, Ryu<sup>1\*</sup> ; ADACHI, Yoshiko<sup>1</sup> ; MIYASHITA, Sumio<sup>1</sup>

<sup>1</sup>Niigata University

It is thought that the ridge segment structure controls partial melting processes of upper mantle and supply system of magmas at the mid-ocean ridges (MacDonald et al., 1988), and we may observe these occurrences at the Oman ophiolite. Fizeh and Salahi blocks of the northern Oman ophiolite is corresponded to the 2nd order ridge segment (Adachi and Miyashita, 2003; Miyashita et al., 2003), wehrlitic intrusions of the near off-axis magmatism are identified different petrological features. The presence of magmatic hornblende is rare in the segment centre but more abundant of hornblende and orthopyroxene at the segment margin (Adachi and Miyashita, 2003; Kaneko et al., 2014). The forsterite content of olivine and the Mg# of clinopyroxene from the wehrlitic intrusions of the segment margin are more evolved than in rocks from the segment centre. Chlorine contents of magmatic hornblende from the segment centre and margin show high contents.

Although Phyton et al. (2007) identified that the seawater penetrates the lower oceanic crust, this study suggests the fluid of seawater implicates magma compositions of near off-axis magmatism. We focus on vertical variations of wehrlitic intrusions, and show the spatial variation of petrographic features and mineral compositions in the along ridge axis, and then perform a three-dimensional study of hydrothermal circulation along the ridge segment structure. It is important to elucidate of the seawater penetrating depth at the oceanic crust formation, we discuss the change in the penetration depth of the seawater along axis, trying to understand of the oceanic crust formation process.

Keywords: near off-axis magmatism, ridge segment structure, wehrlitic intrusion, Oman ophiolite

## Mineralogical characterization of groundmass nanolites in the Shinmoedake 2011 eruption products

MUJIN, Mayumi<sup>1\*</sup>; NAKAMURA, Michihiko<sup>1</sup>; MIYAKE, Akira<sup>2</sup>

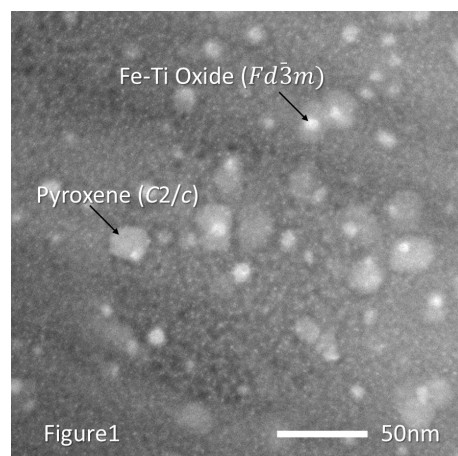
<sup>1</sup>Department of Earth and Planetary Material Science, Graduate School of Science, Tohoku University, <sup>2</sup>Division of Earth and Planetary Sciences, Graduate School of Science, Kyoto University

The groundmass nanolites are submicron scale minerals having a steeper slope of CSD (crystal size distribution) than microlites, originally described for a rhyolitic dome lava (Ben Lomond rhyolite lava dome; Sharp et al., 1996). The nanolites in explosive eruption products were first reported by Mujin and Nakamura (2014) for the pumices and dense juvenile fragments of the Shinmoedake (Kirishima Volcano) eruption in 2011. They found that the mineral assemblage of the nanolites recorded eruption style transition from sub-Plinian pumice, via Vulcanian pumice to lava cap as follows: pyroxene (pyx), pyx + plagioclase (pl), and pyx + pl + Fe-Ti oxides in a descending order of explosivity. In this study, we report their chemical compositions and crystal space groups.

The fine plagioclase microlites in the sub-Plinian pumices have clearly higher An contents (by ca. 5 mol%) than the similarly sized plagioclase (mostly nanolites) in the Vulcanian pumices and lithic fragments. This indicates that the pumices of Sub-Plinian eruption quenched before nanolite nucleation and growth of fine microlite ( $<3 \mu\text{m}$  in width). The decrease in An content from the microlites to the nanolites may be explained by considering two factors: 1) crystallization differentiation of the melt, and 2) decompression and possibly cooling during crystallization.

The compositions of pyroxene nanolites and small microlites ( $1 - 6 \mu\text{m}$  in width), on the other hand, do not show any systematic difference among the eruption styles, being consistent with the CSD results. They were within the metastable compositional range of pigeonite, sub-calcic augite and augite. In the electron diffraction pattern of TEM, we identified the pyroxenes and Fe-Ti oxide crystals as small of 20 and 10 nm in the dense juvenile fragments, respectively. In the HAADF-STEM images (Fig. 1), the pyroxene and Fe-Ti oxide crystals as small as 3 and 1 nm were discernable. Some Fe-Ti oxide crystals were formed on the pyroxene crystal surfaces, suggesting that some of the crystals nucleated heterogeneously. The crystal systems of pyroxene and Fe-Ti oxide nanolites were determined as  $C2/c$  and  $Fd\bar{3}m$ , respectively. This is in contrast to the previously reported pyroxene nanolites in the lava dome sample (Sharp et al., 1996). They were composed of the mixture of orthopyroxene and clinopyroxene, and a complex micro-structure resulting from sub-solidus exsolution from pigeonite ( $P2_1/c$ ) to augite ( $C2/c$ ) and hypersthene. Sharp et al. (1996) interpreted this complexity of pyroxene phases resulted from moderate cooling rate within the obsidian layer. By contrast, we did not confirm the subsistent of the mixed pyroxenes in dense fragments of the Shinmoedake eruption products, because the scale of the observed pyroxene was 1 - 2 orders of magnitude smaller than that of Sharp et al. (1996). The appearance of a metastable phase of pyroxene nanolites and fine nanolites ( $1 - 20 \text{ nm}$ ) in the dense fragments seems to be resulted from the nucleation and growth under large super cooling followed by rapid quenching. The large undercooling may have been produced though rapid magma ascent and succeeding dehydration and liquidus increase, in addition to the cooling and oxidation of the magma near the surface.

Keywords: Nanolite, undercooling, TEM, pyroxene, Fe-Tioxide, plagioclase



## Zircon U-Pb ages of Early Cretaceous igneous rocks in the Kitakami Mountains, Japan

TSUCHIYA, Nobutaka<sup>1\*</sup> ; SASAKI, Jun<sup>1</sup> ; ADACHI, Tatsuro<sup>2</sup> ; NAKANO, Nobuhiko<sup>2</sup> ; OSANAI, Yasuhito<sup>2</sup>

<sup>1</sup>Iwate University, <sup>2</sup>Kyushu University

Early Cretaceous igneous rocks in the Kitakami Mountains consist of volcanic rocks, dike rocks, and plutonic rocks, from older to younger. Plutonic rocks are composed mainly of adakitic granites in central part of zoned plutonic bodies surrounded by adakitic to non-adakitic granites in marginal part. These adakitic plutons is divided into E and W zones based on the ages and geochemistry. Zircon U-Pb ages were determined with laser ablation inductively coupled plasma mass spectrometry (LA-ICP-MS) for 22 samples from 13 rock bodies including the Early Cretaceous adakitic granites in the Kitakami Mountains (Tsuchiya et al., 2015). Zircons from the adakitic granites of E zone give older ages (127–117 Ma) compared with those of W zone (119–113 Ma). Zircon ages become younger from the northern Hashikami pluton and marginal facies of the Tanohata pluton (127–125 Ma) to southern Takase granites (118–117 Ma), in the E zone adakitic granites. Petrochemical differences between the E zone and W zone rocks indicate that the adakitic melt of E zone rocks are considered to be derived from vapor-absent melting condition, while those of W zone rocks are from higher pressure and vapor-present condition. Calc-alkaline to shoshonitic plutonic rocks and dike rocks show narrow range of zircon U-Pb age (128–124 Ma), and are almost contemporaneous to those of the Hashikami, Tanohata, and Miyako plutons (127–125 Ma). Taking all these data into consideration, the Early Cretaceous magmatism in Kitakami can be explained by the differential subduction model of the Farallon-Izanagi plates or slab rollback model accompanied with asthenospheric upwelling.

Keywords: adakite, zircon geochronology, Kitakami, petrochemistry, Cretaceous

## Rock facies of The Hikami granitic body in south Kitakami Mountains, Japan

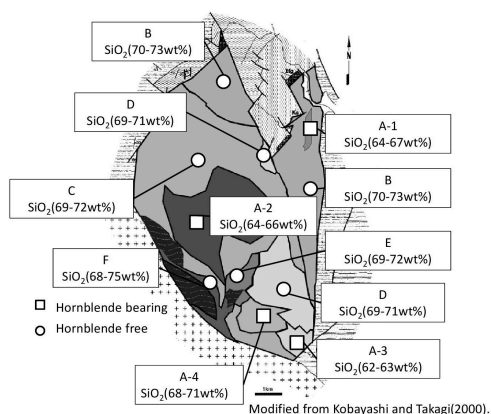
SASAKI, Jun<sup>1\*</sup> ; TSUCHIYA, Nobutaka<sup>1</sup>

<sup>1</sup>Iwate University

The Hikami Granitic Rocks, one of the oldest granites in Japan, crops out from central to eastern part of the South Kitakami Belt. The Hikami Granitic Rocks are distributed mainly around Mt. Hikami, and northern part of small masses. The Hikami Granitic Rocks has long been controversial on their age of intrusion. Sasaki et al. (2013, 2014) examined the zircon U-Pb ages of 13 samples from the Hikami Granitic Rocks, and solidification age of around 450 Ma were obtained.

The Hikami Granitic Rocks were subdivided lithologically into nine types, A-1, A-2, A-3, A-4, B, C, D, E and F on the basis of Asakawa et al. (1999), Kobayashi and Takagi (2000). Petrochemical characteristics of major and minor elements indicate that the Hikami Granitic Rocks are derived from fractional crystallization through a common parental magma.

Keywords: Hikami Granitic Rocks, Petrochemistry, south Kitakami Mountains, Pre-Silurian





## Crystalized melt inclusions in mafic granulite: investigation of partial melting process based on pseudosection

SAITOH, Yohsuke<sup>1\*</sup>; TSUNOGAE, Toshiaki<sup>1</sup>

<sup>1</sup>Yohsuke Saitoh

We report here new petrological date of crystalized melt inclusions (CMIs) and phase equilibrium modeling of partially melted mafic granulite to evaluate the influence of partial melting to the phase relation from the Neoproterozoic - Cambrian Lutzow-Holm Complex (LHC), East Antarctica (Shiraishi et al., 1992). Previous petrological studies of the LHC suggest an increase in the metamorphic grade from northeast (amphibolite facies) to southwest (granulite facies) (Hiroi et al., 1991). CMIs are often reported from the pelitic and felsic granulites (e.g. Cesare et al., 2009). However they are relatively rare in mafic to ultramafic granulites. We thus attempt to investigate textures of the CMIs in the mafic to ultramafic granulites to discuss the partial melting process.

The examined mafic and ultramafic granulites occur as boudin or small blocks of several meters within psammitic and hornblende-biotite gneisses of the granulite-facies zone. Based on detailed microscopic observations, we found CMIs bearing mafic and ultramafic granulites from four different exposures within the LHC. The representative samples of mafic to ultramafic granulite are composed mainly of coarse-grained garnet, hornblende, orthopyroxene, clinopyroxene, plagioclase, and ilmenite. The garnet often contains CMIs. The CMIs consist of fine-grained quartz, orthopyroxene, biotite, K-feldspar, plagioclase, and ilmenite which size varies from 1 to 50 $\mu$ m. The size of CMI grains is up to 100 $\mu$ m, and they show negative crystal shapes of the host garnet. We subsequently calculated chemistry of the CMIs based on modal abundance and chemistry of the minerals for each CMI. The results are nearly equivalent to the compositions of andesitic to dacitic melt.

Occurrence of hornblende and biotite within garnet in the rock suggests dehydration melting of the hydrous minerals and formation of andesitic to dacitic melt during prograde stage. Phase equilibrium modeling in NCKFMASHTO system demonstrated that some mafic to ultramafic granulites experienced considerable amounts of melt loss (up to 6.5-7 wt. %) defined by the stability field of clinopyroxene and modal isopleth of clinopyroxene. Stability field of quartz expands toward lower pressure side with increase of melt amount in the phase diagram. Based on phase equilibrium modeling of melt-bulk interaction, the stability field of quartz and clinopyroxene is critical to estimate the P-T condition and amounts of melt extraction during partial melting. We estimated peak P-T condition of 900 °C and 10-11 kbar and clockwise P-T path for the rock based on the integrated bulk composition. Modal isopleth of the mineral also demonstrated that partial melting progressed through the following reactions.  $Hbl + Bt \rightarrow Liq + Cpx + Grt$ .  $Hbl + Pl \rightarrow Liq + Cpx + Grt$ . This study demonstrated that partial melting took place under plagioclase free field and plagioclase stable field.

The peak condition is comparable with previous estimations of 800-950 °C and 7-12 kbar (Yoshimura et al., 2004). Our results suggest that partial melting and melt loss are common processes even in mafic to ultramafic granulites from the LHC, and CMIs could preserve the composition of melt which has already been extracted from the system. Phase equilibrium modeling suggests that melt loss during prograde stage have critical influence on the mineral assemblage and stability field of the mineral of the examined samples.

### References

- Cesare, B., Ferreol, S., Salvioli, M.E., Pedron, D., Cacallo, A., 2009. *Geology* 37, 627-630.
- Hiroi, Y., Shiraishi, K., Motoyoshi, Y., 1991. *Geological Evolution of Antarctica*, Cambridge University Press, Cambridge, 83-87.
- Shiraishi, K., Hiroi, Y., Ellis, D.J., Fanning, C.M., Motoyoshi, Y., Nakai, Y., 1992. *Recent Progress in Antarctic Earth Science*. Terra, Tokyo, 67-73.
- Yoshimura, Y., Motoyoshi, Y., Miyamoto, T., Grew, S. Edward., Carson, J. Christopher., Dunkley, J. Daniel., 2004. *Polar Geoscience* 17, 57-87.

Keywords: crystalized melt inclusions, mafic granulite, Lutzow-Holm Complex, phase equilibrium modeling

## Chemical Modification of Felsic Melt by Reaction with Peridotite: Implications from the Magarisawa Peridotite, Hokkaido

YAMASHITA, Kohei<sup>1\*</sup>; MAEDA, Jinichiro<sup>2</sup>; YOSHIKAWA, Masako<sup>3</sup>; SHIBATA, Tomoyuki<sup>3</sup>; YI, Keewook<sup>4</sup>

<sup>1</sup>Department of Natural History Sciences, Graduate School of Science, Hokkaido University, <sup>2</sup>Department of Natural History Sciences, Faculty of Science, Hokkaido University, <sup>3</sup>Beppu Geothermal Research Laboratory, Kyoto University, <sup>4</sup>Geochronology Team, Korea Basic Science Institute

It has been well-documented that subduction zone magmatism is induced by partial melting of the hydrated wedge mantle (e.g., Sakuyama, 1982) and/or of subducting slab (e.g., Wyllie and Sekine, 1982). In the latter case, felsic partial melts would have to undergo interaction with peridotites during upward migration through the overriding wedge mantle (e.g., Kay, 1978). However, the detail of felsic melt/peridotite interaction processes has not been fully described due to very rare natural occurrence suitable for petrological examinations (e.g., Shimizu et al., 2004).

We found felsic veins of various size (microscopic order to ca. 50 – 60 cm in width) and with a wide compositional range in the Magarisawa Peridotite (MP), northern Hidaka Mountains, Hokkaido. The MP, one of the mantle peridotite masses situated along the base of the Hidaka Magmatic Belt (Maeda et al., 1986), is mainly composed of Pl lherzolite, and surrounded by pelitic granulites and their anatectic equivalents. Here we present zircon SHRIMP U-Pb age, major element compositions, and <sup>87</sup>Sr/<sup>86</sup>Sr and <sup>143</sup>Nd/<sup>144</sup>Nd isotopic ratios of felsic veins, in order to discuss the chemical modification process of the felsic melts by interaction with mantle peridotite observed in the MP.

On the basis of lithology and whole-rock compositions of the felsic veins, we subdivided them into three facies: (1) Granitic Vein (GV; Qz + Kfs + Pl + Phl + Opx ± Cpx ± Zr ± Ap ± Rtl ± Sph), characterized by higher-SiO<sub>2</sub> (64.0 – 74.5 wt%) and -K<sub>2</sub>O (2.1 – 5.8 wt%), and lower-MgO (0.4 – 2.1 wt%) contents, (2) Pl-veinlet (PV; Plagioclase ± Opx ± Kfs ± Phl ± Zr ± Ap), which is a thin veinlet branched from the GV, (3) Noritic Vein (NV; Pl + Opx ± Phl ± Zr ± Ap ± Fe-Ni sulfide ± Ox), characterized by lower-SiO<sub>2</sub> (55.0 – 60.0 wt%) and -K<sub>2</sub>O (<0.8 wt%), and higher-MgO (2.3 – 6.5 wt%) contents. Although continuous transition between the GV and the NV has not been observed in the field until now, whole-rock composition of the both veins represent a single trend on the Harker diagram. The PV is intermediate on the trend between the GV and the NV.

Orthopyroxenite (0.5 – 1.5 mm in thickness) composed of mosaic-shaped secondary Opx with subordinate amounts of Phl is always observed along the vein/peridotite boundary, clearly suggesting that the veins were formed from SiO<sub>2</sub>-oversaturated melts and reacted with Ol in peridotites (e.g., Sen and Dunn, 1994). Furthermore, the microscopic/microprobe analyses indicate that secondary Opx is also formed by reaction between the felsic melts and primary Opx, Cpx, and Spl in the host lherzolite.

Zircon U-Pb age of the Noritic Vein is 19.5 ± 0.25 Ma, which corresponds to one of the main phases of the Hidaka magmatism and metamorphism (e.g., Maeda et al., 2010).

<sup>87</sup>Sr/<sup>86</sup>Sr initial ratios of GV, PV and NV are 0.70531 – 0.70550, 0.70541 – 0.70551 and 0.70560 – 0.70566, respectively, and <sup>143</sup>Nd/<sup>144</sup>Nd initial ratios of them are 0.51258 – 0.51260, 0.51260 – 0.51261, 0.51245 – 0.51260, respectively. Isotopic compositions of all felsic veins are apparently similar to those of the pelitic granulite/anatexite surrounding the MP (Maeda and Kagami, 1996).

Because formation of Opx from Ol consumes SiO<sub>2</sub> in the melts, the successive melt should become less-silicic, indicating the continuous modification of the melt composition from the GV through the PV to the NV. We have performed simple mass balance calculations to derive the NV from GV for major element composition. The results show that the composition of the NV can be modeled by addition of Ol, Cpx and Spl (in the host peridotite) to and subtraction of Opx and Phl (in the orthopyroxenite) from the GV.

In summary, we propose that the felsic veins within the MP record a significant chemical modification of SiO<sub>2</sub>-oversaturated felsic melt during the interaction with mantle peridotite.



## Characteristics of chromitites from the Higashi-akaishi ultramafic complex: Implications for origin of UHP chromitite

MIURA, Makoto<sup>1\*</sup> ; ARAI, Shoji<sup>1</sup> ; MIZUKAMI, Tomoyuki<sup>1</sup> ; YAMAMOTO, Shinji<sup>2</sup> ; VLADIMIR, Shmelev<sup>3</sup>

<sup>1</sup>Department of Earth Sciences, Kanazawa University, <sup>2</sup>Department of Earth Science and Astronomy, University of Tokyo, <sup>3</sup>Institute of Geology and Geochemistry, Ural Branch Russian Academy of Sciences

Ultrahigh-pressure (=UHP) chromitites, which contain UHP minerals such as diamond and coesite, have been observed from ophiolites in Tibet and the Polar Urals. However, their nature, i.e. origin, frequency of appearance and P-T path, are still controversial because of insufficiency of detailed petrographic studies. Systematic observation and classification of various chromitites and enclosing peridotites from some localities are required.

Chromitites in the Higashi-akaishi ultramafic complex in the Cretaceous Sanbagawa metamorphic belt, Japan, is one of keys to interpret the origin of UHP chromitite. The Higashi-akaishi ultramafic complex is characterized by the presence of garnet in some peridotites and pyroxenites, and interpreted as a high-P metamorphic (up to 3.8 GPa) complex originally formed at a lower-P subduction zone mantle. The chromitites in the Higashi-akaishi ultramafic complex had also experienced the high-P metamorphism. They will provide us with information on the behavior of low-P chromitite upon compression via subduction.

Spinel in the Higashi-akaishi chromitite contains various inclusions, i.e. numerous needle- and blade-like diopside lamellae, and is free of primary inclusions of hydrous minerals, such as pargasite and Na phlogopite. Solid-phase secondary inclusions are mostly composed of chlorite and serpentine. Chromian spinels in the Higashi-akaishi chromitite show high Cr#s (0.8 to 0.85) and low Ti contents (<0.1 wt%), suggesting an arc-related feature. Spinel in the Higashi-akaishi chromitite and surrounding peridotite were sometimes fractured by deformation.

The Higashi-akaishi chromitite is similar in features of inclusions in spinel and spinel chemistry to the UHP chromitites from Tibet and the Polar Urals. This similarity suggests that some of the characteristics of the UHP chromitite can be formed by compression of low-P chromitite, e.g., recycling via a subduction zone. In addition, such diopside lamellae in spinel of the Higashi-akaishi chromitite are typically found from some low-P chromitites from the Oman ophiolite and the Iwanai-dake ultramafic complex, Japan. Their occurrence suggests that the UHP Ca-ferrite (or Ca-titanite) type spinel precursor is not a prerequisite for exsolution of silicate lamellae.

Keywords: Podiform chromitite, The Higashi-akaishi ultramafic complex, Spinel, Exsolution lamella, Ultrahigh-pressure chromitite

## Phase transition of sillimanite with Al/Si-disordering at high temperature

IGAMI, Yohei<sup>1\*</sup>; KOGISO, Tetsu<sup>2</sup>; OHI, Shugo<sup>1</sup>; MIYAKE, Akira<sup>1</sup>

<sup>1</sup>Kyoto Univ., Sci., <sup>2</sup>Kyoto Univ., HES.

Naturally occurring polymorphs of  $\text{Al}_2\text{SiO}_5$  (andalusite, kyanite, sillimanite) have assumed a special significance for geologists because of their value as indicators of the pressures ( $P$ ) and temperatures ( $T$ ) experienced by metamorphic rocks. Especially, sillimanite may have more geological information in its crystal structure or microstructure. For example, it has been indicated experimentally that sillimanite show the structures like anti-phase boundaries (APB) and/or enrich to Al releasing  $\text{SiO}_2$ -rich melt at high temperature (Holland & Carpenter, 1986). Miyake et al. (2008) showed sillimanite in Napier complex has APB-like structure and fine mullite inclusion (which is more Al-rich than sillimanite,  $\text{Al}_2[\text{Al}_{2+2x}\text{Si}_{2-2x}\text{O}_{10-x}]$ ). In addition, Greenwood (1972) suggested the phase of completely Al/Si-disordered sillimanite as another phase from sillimanite. And, Fischer et al. (2014) found new phase different from sillimanite, mullite, and “completely Al/Si-disordered sillimanite”. These phase also can be valuable geological indicator, but their behaviors are not clear. They need very high resolution for analysis to be detected and classified. Like this, phase relation of sillimanite at high  $T$  (and high  $P$ ) is still so confused. In this study, synchrotron powder X-ray diffraction (XRD) and transmission electron microscope (TEM) experiments were carried out on samples of sillimanite heat-treated in various conditions ( $P$ ,  $T$  and duration time) in order to clarify behavior of sillimanite at high temperature.

We heated sillimanite ( $\text{Al}_{2.00}\text{Si}_{0.99}\text{Fe}_{0.01}\text{O}_5$ ) crystals in Rundvagshetta, Lutzow-Holm, Antarctica.sillimanite in the range of 0.8-2.5GPa, 1000-1500 °C for 10-1751 hours and then quenched. Experimental products (46 samples) were examined by Synchrotron powder XRD experiment at BL-4B<sub>2</sub> in photon factory, KEK and observed TEM (JEOL JEM-2100F) from the viewpoint of  $l$ -odd reflections (which distinct with Al/Si-disordering) and chemical composition.

As a result of XRD experiments, the diffraction patterns of mullite were observed in many samples. Moreover, in four samples heated at 1300-1400 °C, 1GPa, the peaks of unknown phase were observed in addition to that of sillimanite and mullite. This phase have an intermediate feature between peaks of sillimanite and mullite. (So, we will call it “intermediate-phase” .) As a result of TEM observation of these four samples, grains of the intermediate-phase did not give  $l = \text{odd}$  reflections, which are characteristic of sillimanite, but distinct with Al/Si-disordering. By chemical analysis (TEM-EDS), the intermediate-phase was slightly Al-rich more than sillimanite but less than mullite. So, It was revealed that the intermediate-phase has the structure which has disordered distribution of Al/Si on the tetrahedral sites, with releasing very little  $\text{SiO}_2$  from  $\text{Al}_2\text{SiO}_5$ . This phase can be stable at high temperature and 1GPa. The intermediate-phase is probably not same as “completely Al/Si-disordered sillimanite” by Greenwood (1972) etc., but may be same as the new phase founded by Fischer et al. (2014). The sillimanite with APB and fine mullite inclusion by Miyake et al. (2008) can be explained as that sillimanite transformed from intermediate phase with mullite. APB was made by Al/Si-ordering when intermediate phase transformed to sillimanite.

### References:

- [1]Holland & Carpenter (1986) Nature, 320, 151-153
- [2]Miyake et al. (2008) JAMS Annual Meeting Abstract
- [3]Greenwood (1972) THE Geological Society of America, 132, 553-571
- [4]Fischer et al. (2014) IMA General Meeting Abstract, 21, 335

Keywords: sillimanite, mullite, Al/Si-disordering, synchrotron X-ray experiment

## Size effect on the phase transition between protoenstatite and clinoenstatite

OSAKO, Tatsuya<sup>1\*</sup> ; OHI, Shugo<sup>1</sup> ; IGAMI, Yohei<sup>1</sup> ; MIYAKE, Akira<sup>1</sup>

<sup>1</sup>Kyoto Univ. Sci.

### [Introduction]

Protoenstatite(PEN, space groupe:*Pbcn*), one of the polymorph of enstatite( $MgSiO_3$ ), is the stable phase at high temperature above 1000 °C below 1557 °C at atmospheric pressure. It is generally known that protoenstatite is the unquenchable phase. Actually, PEN has never been reported from natural specimens to date. However, Foster (1951), Lee and Heuer(1987), and so on reported PEN was observed at room temperature from experimental generative materials.

Smyth(1974) studied in detail the transformations among polymorphs of enstatite using high temperature single-crystal X-ray techniques. He showed that in rapid quench PEN transformed to clinoenstatite(CEN,  $P2_1/c$ ) and in slow cooling rate PEN transformed to orthoenstatite(OEN, *Pbca*), and concluded that the rapid transformation between PEN and CEN occurs martensitically. On the martensitic transformation, in general, it is known that the transformation starting temperature is effected by the grain size that is i.e. the smaller grain has the lower starting temperature.

It is inferred that grain size affect the PEN-to-CEN transformation because the transformation is considered martensitic. The purpose of this study is to make clear the condition PEN can retain at room temperature which associated with grain size.

### [Experiments]

The starting material of experiments was OEN synthesized by the flux method according to Ozima(1982). We crushed and as-sorted synthetic OEN as grain size ( $\sim 3\mu m$ ,  $\sim 10\mu m$ ,  $35\sim 51\mu m$ ,  $32\sim 63\mu m$ ,  $51\sim 73\mu m$ ,  $73\sim 96\mu m$ ,  $63\sim 125\mu m$ ,  $96\sim 105\mu m$ ), and heated these samples by the box electric furnace at 1200 °C for 20 hours, and after that cooling rate was 5 °C/min. And furthermore at the synchrotron radiation institution Photon Factory we examined the in situ observation of the PEN to CEN transformation at high temperature to obtain the transformation starting temperature.

### [Results]

Only CEN peaks existed in the larger sample than  $73\sim 96\mu m$ , on the other hand both CEN and PEN peaks existed in the smaller than  $51\sim 73\mu m$ . In  $73\sim 96\mu m$  sample the PEN to CEN transformation started at about 700 °C, however in the  $\sim 3\mu m$  sample the transformation started at about 600 °C. These results indicate that the grain size evidently affect the phase transition temperature between PEN and CEN, that is, the PEN-to-CEN transformation is martensitic. Furthermore these suggest that PEN can retain at room temperature if its size is on the order of several  $10\mu m$  and less.

[1]Foster(1951), *J. Am. Ceram. Soc.* 34 [9], 255-259.

[2]Lee end Heuer(1987), *J. Am. Ceram. Soc.* 70 [5], 349-360.

[3]Ozima(1982), *Ganseki Koubutsu Kousyogaku Gakkaishi Tokubetsugo*(Japanese) 3, 97-103.

Keywords: enstatite, phase transition, size effect

## Mineral chemistry of anorthite megacryst and its inclusions from Mt. Fubo, Minami Zao

ECHIGO, Takuya<sup>1\*</sup>; NISHIMAKI, Shino<sup>2</sup>; TANIGUCHI, Naoki<sup>1</sup>; KIMATA, Mitsuyoshi<sup>3</sup>; SHIMIZU, Masahiro<sup>3</sup>; SAITO, Shizuo<sup>4</sup>; NISHIDA, Norimasa<sup>5</sup>

<sup>1</sup>Faculty of Education, Shiga University, <sup>2</sup>Master's Program in Science and Engineering, University of Tsukuba, <sup>3</sup>Doctoral Program in Earth Evolution Sciences, University of Tsukuba, <sup>4</sup>Institute of Materials Science, University of Tsukuba, <sup>5</sup>Research Facility Center for Science and Technology, University of Tsukuba

Anorthite megacrysts, which are high-calcic plagioclase (An >90 mol%) phenocrysts larger than 10 mm, are characteristic minerals occurring in basalt - andesite from Japanese Islands arc (Kimata et al. 1995). Anorthite megacrysts from Miyakejima contains various inclusions such as native copper (Cu: Murakami et al. 1991), native zinc (Zn: Nishida et al. 1993) and native brass (Zn-Cu alloy: Nishida et al. 1993). In addition, hydrocarbon was also reported from Miyake-jima anorthite (Kimata et al. 1993), which suggests that slab sediments on subducting plates had important role for crystallization of these anorthite megacrysts. These past studies indicate that mineral, melt or liquid inclusions in anorthite megacrysts may afford a clue to the formation process of such minerals. We report the analytical results of sulfide inclusions in anorthite megacrysts from Mt. Fubo (one peak of Minami Zao volcanos). Mt. Fubo is located along the volcanic front and the anorthite megacryst occurs in lavas erupted in the Quaternary period. The chemical analyzes of the anorthite megacrysts (host crystal) and sulfide inclusions were carried out using an electron microprobe analyzer with wavelength dispersive X-ray spectroscopy (EMPA-WDS: JEOL JXA-8230) and/or a scanning electron microscope with energy dispersive X-ray spectroscopy (SEM-EDS: J JEOL JXA-8230). The analytical results show that the anorthite megacrysts from Mt. Fubo contain sulfide inclusions that are droplet-shaped and 30 - 50 micrometer in diameter. The chemical compositions of the sulfide inclusions in anorthite megacrysts are heterogeneous; Fe-rich phase and Cu-rich phase were observed within a single inclusion. Quantitative analyzes suggest that the Fe-rich phase is pyrrhotite [ $\text{Fe}_{(1-x)}\text{S}$  ( $x=0-0.17$ )] and Cu-rich phase is cubanite ( $\text{CuFe}_2\text{S}_3$ ), respectively, and these phases contain both Ni and Cu. These sulfide inclusions consisting the two phases may be trapped as fluid inclusions in the host crystals (anorthite megacrysts) at high temperature. The trapped sulfide liquids seem to be separated from silicate melts as monosulfide solid solution ( $\text{Fe}_{(1-x)}\text{S}$ - $\text{Ni}_{(1-x)}\text{S}$ : Naldrett et al. 1967) or intermediate solid solution ( $\text{CuFeS}_2$ : Fleet 2006) and exsolved into pyrrhotite and cubanite in the host crystals upon cooling. The present study indicates that sulfide melts rich in Fe, Cu and Ni were generated within magmas along the volcanic front in Japan.

Keywords: Anorthite, Arc magma, Sulfide, Inclusion

## Texture and formation process of jasper, "Nishiki-ishi" from Tsugaru region, Japan

ISHIKAWA, Shiori<sup>1\*</sup>; NAGASE, Toshiro<sup>2</sup>; KURIBAYASHI, Takahiro<sup>1</sup>

<sup>1</sup>Institute of Mineralogy, Petrology and Economic Geology, Graduate School of Science, Tohoku University, <sup>2</sup>The Tohoku University Museum

Jasper with bright red, yellow and green colors occurs from Tsugaru region, Aomori prefecture, Japan, and is called as "Nishiki-ishi" from its coloring. The jasper is used for ornaments at the region. The colors originate from iron-containing minerals within the jasper. Most raw stones of Nishiki-ishi are usually collected from shingle at beach, and few outcrop of the jasper is found out. Therefore, the occurrence of Nishiki-ishi has not been reported in detail. To elucidate the formation process of Nishiki-ishi, we observed textures of rocks and minerals, and analyzed the chemical compositions of minerals.

Used samples were collected from two localities: Aoiwa, Nakadomari-machi, Kita-tsugaru, Aomori prefecture, and Tappi-zaki, Sotogahama, Higashi-tsugaru, Aomori prefecture, Japan. Both localities are located in the green-tuff regions of Miocene, and are underlain by pyroxene andesite rocks (Tappi andesite) with volcanic breccia. Silica veins of quartz, chalcedony and opal are locally developed within the rock. Nishiki-ishi mainly consists of quartz and iron-containing minerals, and other minor minerals are barite, apatite and ankerite.

The textures of rocks and minerals were observed using an optical microscope and a scanning electron microscope (JEOL, JSM-7001F), and chemical analyses were carried out using an energy dispersive X-ray analyzer (Oxford, INCA system).

Quartz crystals composing Nishiki-ishi exhibit fibrous spherules with 0.1 mm in diameter or aggregations of micro-crystals with 0.05 mm in width. Comparing with chalcedony and agate, Nishiki-ishi has coarser fibers in the quartz spherules and few zonal-band texture. Origin of its colors is caused by iron-containing minerals; hematite (red), celadonite (green), goethite (yellow), siderite (yellow), pyrite (brown). These iron-containing minerals, which exhibit needle-like or granular forms, are included as fine grains in quartz spherules and fill in space among the quartz spherules.

The macroscopic structure of Nishiki-ishi is a breccia-like or clastic. The breccia fragments consist of aggregates of micro-quartz and optically length-slow types spherules. In contrast, the space among these breccia fragments is filled by clearly euhedral quartz crystals and chalcedony with optically length-fast. These are considerable differences of quartz textures between breccia and the space among of breccia fragments. The original rock of Nishiki-ishi was formed by silicification of volcanic rocks during volcanic activity. After the silicified rocks brecciated, quartz and chalcedony precipitates in the breccia.

Keywords: jasper, Nishiki-ishi, chalcedony, texture

## New occurrence and mineralogical properties of rhabdophane group minerals from Higashimatsuura basalt, Kyushu, Japan

UEHARA, Seiichiro<sup>1\*</sup>; SHOBU, Ayaka<sup>1</sup>; TAKAI, Yasuhiro<sup>2</sup>; SHIROSE, Yohei<sup>1</sup>

<sup>1</sup>Dep. Earth & Planet. Sci. Kyushu Univ., <sup>2</sup>Enecom Co., Ltd.

### 1. Introduction

Higashimatsuura basalt is the alkali olivine basalt distributed in the northwest of Saga Prefecture, Japan. Many rare earth minerals including five new rare earth minerals, kimuraite-(Y) (Nagashima et al., 1986), kozoite-(Nd) (Miyawaki et al., 2000), kozoite-(La) (Miyawaki et al., 2003), hizenite-(Y) (Takai and Uehara, 2013) rhabdophane-(Y) (Takai and Uehara, 2012), were found in the basalts. It is very rare locality that rare earth minerals are found in basalts.

Rhabdophane, (REE) PO<sub>4</sub> • H<sub>2</sub>O (REE = La, Ce, Nd, Y), is a hydrous rare earth phosphate mineral. Rhabdophane commonly occurs as a secondary mineral replacing monazite in syenite, alkali syenite pegmatite and sedimentary rock. Recently, many synthetic studies of rhabdophane group minerals are reported for industrial application (e.g., Mesbah et al., 2014). Some rhabdophane which do not found in nature are also synthesized; rhabdophane-(REE) (REE = La, Ce, Pr, Nd, Sm, Gd, Tb, Dy, Y, Er, Yb, Lu) are made (Hikichi et al., 1989; Min et al., 2000). However, detailed occurrence studies of rhabdophane in the nature have not been well investigated.

Takai and Uehara (2012) reported rhabdophane-(Y) as a new mineral from Hinodematsu located in the center of Higashimatsuura peninsula. However, its detailed occurrence of rhabdophane species and their chemical variations were not reported. This paper reports the occurrence, distribution and mineralogical features of rhabdophane group minerals from Hinodematsu and their distribution in Higashimatsuura peninsula.

### 2. Analysis method

Nineteen samples (H01-H19) were collected from the Higashimatsuura basalt in Hinodematsu. All samples were prepared as several thin sections, and the existence of rare earth minerals were investigated and carried out chemical analyses by scanning electron microscope with EDS (JEOL JSM-5800LV SEM-EDS and JEOL JEM7001F FE-SEM). In some samples, mineralogical features of rare earth phosphates were investigated by SEM (JEOL JSM7001F and Carl Zeiss GEMINI URTRA55 FE-SEM), X-ray diffraction (Rigaku RINT RAPIDII) and scanning/transmission electron microscope (JEM-ARM 200F TEM/STEM).

### 3. Result and Discussion

#### (1) Rare earth phosphates from Hinodematsu

Rhabdophane group minerals are found in cavities of the basalts as two types of occurrence at Hinodematsu (Fig.). One is spherical type which is an isolated relatively large spherical (or radiated) crystal with more than 50 μm in diameter composed of very small rhabdophane hexagonal prismatic crystals of few hundreds nm in width. The other is coating type which is aggregated spherical crystals, the size of each spherical crystal is relatively small with one to 10 μm in diameter. Five rare earth phosphates were observed in these two types of spherulites; rhabdophane-(La), rhabdophane-(Nd), rhabdophane-(Ce), rhabdophane-(Y) and xenotime-(Y) like mineral. Chemical compositions of rhabdophane vary widely in one sample. The Nd/La ratios of rhabdophane were constant in one sample and the amount of Y was different. The Nd/La ratios in all samples were divisible into two types, which is Nd-rich type and La-rich type. Rare earth phosphates from Hinodematsu often occur with chemical zoning as coating type and spherical type. In zoning structure, Nd-rich type occurs as spherical type and La-rich type occurs as coating type. Hinodemastu was unique area where many species of rhabdophane group minerals with chemical zoning are found in the alkali olivine basalts.

#### (2) Rhabdophane group minerals from Higashimatsuura peninsula

Rhabdophanes from Higashimatsuura peninsula are found in several localities and have wide chemical composition as same as the variation found in the Hinodematu rhabdophane group minerals. Rhabdophane-(Ce) is also found. Therefore, rhabdophane group minerals from Hinodematsu and Higashimatsuura peninsula should be primary minerals formed by late stage, low temperature hydrothermal mineral in REE rich alkali basalts.

Keywords: rhabdophane group minerals, rhabdophane-(Y), hydrous rare earth phosphate mineral, Higashimatsuura basalt, Hinodematu



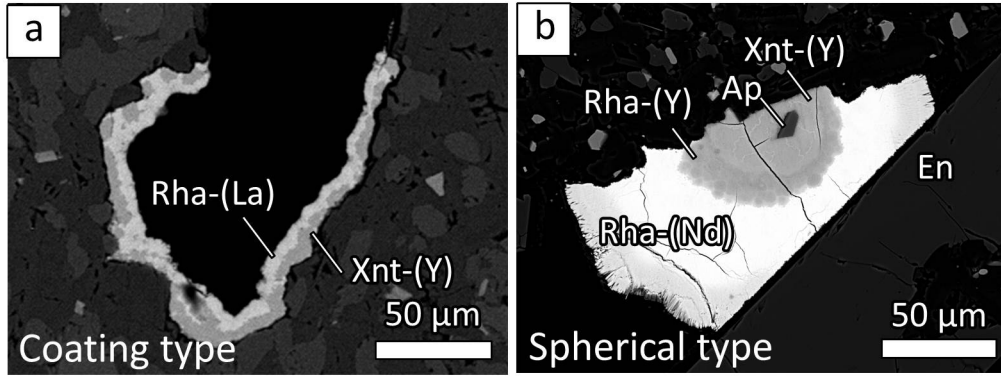


Fig. BSE images of REE phosphates with chemical zoning structure. (a) Cavity coated with rhabdophane-(La) and xenotime-(Y) like minerals (sample H06). (b) Sphere of REE phosphates with zoning structure consisted of rhabdophane-(Nd), rhabdophane-(Y) and xenotime-(Y) like mineral (sample H07).

## X-ray CT and Raman spectroscopy analyses of polyphase fluid inclusions of quartz crystals from Tsushima granite

FUJIMOTO, Kyouzuke<sup>1</sup> ; MIYAKE, Akira<sup>1\*</sup> ; TSUCHIYAMA, Akira<sup>1</sup> ; NAKANO, Tsukasa<sup>2</sup> ; UESUGI, Kentaro<sup>3</sup> ; YOSHIDA, Kenta<sup>1</sup> ; MATSUNO, Junya<sup>1</sup> ; KUROSAWA, Masanori<sup>4</sup>

<sup>1</sup>Kyoto Univ., <sup>2</sup>AIST, <sup>3</sup>JASRI, <sup>4</sup>Tsukuba Univ.

Tsushima granite and the related rocks, southwestern Japan, are known for abundant aqueous polyphase inclusions with large daughter crystals of halite, sylvite, and carbonate. Kurosawa et al. (2012) analyzed chemical compositions of the polyphase fluid inclusions in quartz from miarolitic cavities at Tsushima granite with particle-induced X-ray emission (PIXE), and Kurosawa (2014) directly observed and analyzed the daughter minerals denuded by fracturing the quartz host by using SEM-EDS and identified the phase with Raman microspectroscopy. However, the three dimensional distribution and the morphology of daughter minerals, and the volumes of solid, liquid and vapor phases could not be revealed. Furthermore, it has the potential to transit for daughter mineral to another phase because of the dehydration and so on at fracturing the host to open the inclusion. On the other hand, X-ray computed tomography (XCT) method is the non-destructive analysis and provides the various three dimensional information such as the morphology and the volume. Recently, a linear attenuation coefficient (LAC), which depends on mass density, chemical composition and incident X-ray energy, can be calculated by the synchrotron radiation XCT (SR-XCT) and mineral phase can be inferred from the LAC value. In the present study, we analyzed the polyphase fluid inclusions in quartz crystals from a miarolitic cavity at the Tsushima granite with SR-XCT, Raman microspectroscopy, and SEM-EDS to identify the daughter mineral phases and estimate the chemical composition of daughter minerals and the liquid phases and volume ratios of solid, liquid and vapor phases.

Results from SR-XCT and Raman spectroscopy of two polyphase-inclusion samples, 1A and 1B, show presence of daughter crystals of halite, sylvite, saltonseaitite (K<sub>3</sub>NaMnCl<sub>6</sub>) siderite, and Fe-OH mineral (goethite?) in the inclusions. The crystals of saltonseaitite, siderite, and Fe-OH mineral, were not reported by the previous SEM-EDS observations (Kurosawa, 2014). Saltonseaitite was first reported by Kampf et al. (2013) and was first observed in Japan. In addition, crystals of calcite and Fe-Cl mineral reported by Kurosawa (2014) could not be observed in this study. The calculated LAC from liquid phase value has the larger value than that calculated from the saturated solution of NaCl or KCl. Thus, it needs to add about 8 mol% Fe to saturated solution of NaCl. We also estimated the volume ratios of the solid, liquid and vapor phases and the bulk chemical composition of each sample. The ratio of vapor to whole inclusion had different values between two neighboring polyphase-inclusions, although the ratios of solid and liquid phases and bulk chemical composition were almost the same. This suggests the possibility that these inclusions had been captured at the different period, because fluid inclusions formed at the same generation have usually almost the same volume ratios among vapor and liquid phases. Furthermore, we dug in the quartz to directly observe and analyze the daughter phase in other polyphase-inclusion sample using focused ion beam. Daughter crystals of hematite and unknown phases, which could not be detected in XCT samples, were observed. Because there is a possibility of transiting from Fe-OH mineral observed by XCT and Raman spectroscopy to hematite in vacuum condition.

Kurosawa et al. (2012) 2012 Annual meeting Japan Association of Mineralogical Sciences (Japanese), Kurosawa (2014) 2014 Annual meeting Japan Association of Mineralogical Sciences (Japanese), Kampf et al. (2013) *American Mineralogist*, 98, 231.

Keywords: polyphase fluid inclusion, X-ray CT, Raman spectroscopy, phase identification